Indian Journal of Chemistry
Vol. 53A, June 2014, pp. 665-671

Preparation, characterization and photocatalytic activity of cerium-doped titanium dioxide supported on activated carbon fiber composite

Shuhua Yao, Yue Yang, Shuangping Song & Zhongliang Shi*

School of Applied Chemistry, Shenyang University of Chemical Technology, Shenyang 110142, China
Email: shzhl2000@163.com

Received 29 October 2013; revised and accepted 22 April 2014

A visible light-driven photocatalyst, viz., Ce/TiO_2/ACF, has been prepared by supporting the photoactive cerium-doped titanium dioxide on activated carbon fibers via hydrolysis of tetrabutyl titanate with ammonium ceric nitrate in the presence of activated carbon fibers. TiO_2 is used for photocatalysis while the activated carbon fibers is used for separation and the doped cerium is used to enhance the photocatalytic activity of titanium dioxide. The prepared photocatalysts have been characterized by BET surface area, scanning electron microscopy, X-ray diffraction and UV-vis absorption spectroscopy. The effect of cerium-doped content on the photocatalytic activity has been studied and 0.2 mol% Ce/TiO_2/ACF is found to exhibit the highest photoactivity. The photocatalytic activities of the obtained photocatalysts under UV and visible light have been estimated by measuring the degradation rate of methylene orange in aqueous solution. Results show that the prepared photocatalyst is activated by visible light and may be used as effective catalyst in photooxidation reactions. In addition, the recyclability of the prepared photocatalyst is also confirmed since the Ce/TiO_2/ACF retains *ca.* 86.5% of its activity after being used four times. The photocatalyst, therefore, may be potentially applied for the treatment of water contaminated by organic pollutants.

Keywords: Photocatalysts, Supported catalysts, Doped catalysts, Cerium doping, Dye degradation, Titanium dioxide, Activated carbon fiber composites

Titanium dioxide (TiO_2), an inexpensive, non-toxic and biocompatible material, has been extensively used in environmental applications for its high activity, chemical stability and robustness against photocorrosion, especially for the detoxification of water and air[1-4]. However, in field applications, there are at least two obvious problems arising from using fine titanium dioxide powders, i.e., (1) low photoefficiency, and, (2) separation of fine particles of TiO_2 used after the treatment process and the recycling of the photocatalyst[5]. In order to improve the photocatalytic activity of fine TiO_2 powders, many studies[6-13] have been carried out, which showed that selective metal ion doping is an effective method to improve the photocatalytic efficiency of this material. Rare earth metals having incompletely occupied 4*f* and empty 5*d* orbitals often serve as catalyst or catalysis promoter. Studies have shown that the photocatalytic activity of TiO_2 can be improved by doping with some rare earth metals[14-16]. Xie *et al.*[15] reported the visible light induced photodegradation of X-3B by cerium modified titania sol and nanocrystallites. Liu *et al.*[17] showed that the CeO_{2-y}-TiO_2 ($0<y<0.5$) powders may apparently shift the UV absorption band of TiO_2 towards visible range. Many techniques have been proposed for the immobilization of fine TiO_2 on solid supports to eliminate the second problem[18-21]. However most of the substrate materials used are granule-shaped, which may significantly limit the efficiency of photocatalyzed oxidations since most of the TiO_2 loaded in the pores is not available for photon irridiation.

Activated carbon fiber (ACF) is a highly microporous carbon material, and has much larger external surfaces than the granular activated carbon (GAC). This makes it an ideal candidate as supporting material for TiO_2. There are many reports in literature on the preparation of loaded TiO_2 on cotton fibers and cellulose fibers[19,22] and transition metal and non-metal doping of TiO_2 particles. To the best of our knowledge, doping of rare earth metals, particularly cerium, in TiO_2 and synthesis of ACF supported Ce-doped TiO_2 and its application to photocatalytic oxidation of methylene orange in aqueous solution have not been reported so far. In the present study, a series of Ce/TiO_2/ACF composites (Ce/TiO_2 supported on ACF) were prepared by sol-gel-

adsorption method via the hydrolysis of $Ti(OBu)_4$ with ammonium ceric nitrate in the presence of activated carbon fibers. The photocatalytic activity of Ce/TiO_2/ACF was evaluated by photodegradation of MO over the obtained samples under UV and visible light irradiation. The objective of this work was to prepare the supported photocatalyst Ce/TiO_2/ACF and to investigate its properties and the possibility of recyclability of the prepared photocatalyst.

Materials and Methods

All the chemicals used in the study were of analytical grade. All the solutions in the study were prepared using de-ionized water. All glasswares were cleaned by rinsing with hydroxylamine hydrochloride, soaking in 10% HCl, and rinsing with de-ionized water.

Viscose rayon-based carbon fibers in felt form used in this study were supplied by Zichuan Carbon Fiber Co. Ltd (China). The fibers were repeatedly treated with boiling de-ionized water until the *p*H of the solution remained unchanged, then dried overnight at 80 ºC and cooled in a desiccator.

Synthesis of photocatalysts

Anatase TiO_2 was prepared by a sol-gel method at low temperature using tetrabutyl titanate ($Ti(OBu)_4$, Analytic grade, Shanghai Xingta Co. Ltd, China) as precursor. $Ti(OBu)_4$ (0.02 mol) was added to anhydrous ethanol (50 mL) under vigorous stirring conditions and then triethylamine (0.01 mol) was added as a stabilizer of the solution and stirred (200 r/min) for 2–3 min under an inert environment, with N_2 flow through the system. A second solution was then prepared separately as follows: hydrochloric acid (3.0 mL) and water (0.72 mL) were added to anhydrous ethanol (50 mL) and mixed well by a magnetic stirrer (200 r/min). The two solutions were then mixed together and stirred vigorously for 30 min under N_2 flow. The formed TiO_2 sol was transparent, quite stable and highly sensitive to the amount of triethylamine and water. For the impregnation, several pieces of ACF, after being dried in a preheated oven, were immersed for 1 h in the TiO_2 containing liquid sol. The titanium sol/ACF turned into titanium gel/ACF after aging for 7 days at 25 ºC. The TiO_2/ACF catalyst was obtained by desiccation of the titanium gel/ACF system at 100 ºC for 6 h and then calcined at 500 ºC in a N_2 atmosphere for 2 h.

Ce-doped TiO_2/ACF was synthesized using the same method. The appropriate content of ammonium ceric nitrate was dissolved in anhydrous ethanol, which was added dropwise into the distilled water, prior to the hydrolysis of $Ti(OBu)_4$ under vigorous stirring.

Characterization of photocatalysts

The specific surface area and pore volumes of samples were obtained by nitrogen adsorption-desorption at 77 K using the BET method with a Micromeritics 2000 instrument (ASAP 2000, Micromeritics, USA). The micrographs of the prepared samples were examined with a scanning electron microscope (SEM, Holland Philips, JSM-5800). The crystalline phases of all the prepared samples were analyzed on a Rigaku D/max-r B X-ray diffractometer with Cu-Kα radiation in the scanning range of 2θ between 20º and 80º. The accelerating voltage and applied current were 40 kV and 30 mA, respectively. Data were recorded at a scan rate of $0.02^{o}\cdot s^{-1}$ in the 2θ range of 20º–80º. UV-vis absorption spectroscopic measurements were made using a UV-vis diffuse reflectance spectrophotometer (Shimadzu UV-2550). Reflectance spectra were referenced to $BaSO_4$. The band gap energies (Eg) of the prepared photocatalysts was calculated by the formula $Eg = 1239.8/\lambda g$ from the wavelength values corresponding to the intersection point of the vertical and horizontal parts of the spectra (λg)[23].

Photocatalytic degradation studies

Methylene orange (MO), a representative substance of dye compounds, was chosen as model pollutant and the degradation of MO (50 mg/L) was used to evaluate the photocatalytic performance of the obtained samples under UV and visible light irradiation.

UV light irradiation

Experiments were carried out using a magnetically stirred quartz reactor and an ultraviolet mercury lamp (150 W, 365 nm) at ambient temperature of *ca*. 20 °C. Ce/TiO_2/ACF (0.2 g) was added to the reactor filled with 100 mL MO aqueous solution (50 mg/L). The *p*H of the suspension was adjusted either with dilute 0.1 mol/L HCl or 0.1 mol/L NaOH. Adsorption time of 60 min in dark condition was allowed before start of the photoreaction. Samples of the suspension were withdrawn after a definite time interval and filtered through 0.22 μm filter paper to remove the catalyst particles. Then, the residual MO concentration was analyzed using a UV-vis spectrophotometer (UV762, Shanghai Analysis Co.). For comparison, the

photocatalytic activities of the pure TiO_2 powders and TiO_2/ACF were also studied. The amount of TiO_2 powder and TiO_2/ACF was 2.0 g/L each, which was adequate under the present experimental conditions. The Ce/TiO_2/ACF sample was used repeatedly, each cycle lasting 4 h. Before the beginning of the next cycle, the remaining solution was replaced by fresh MO solution (50 mg/L).

Visible light irradiation

The experiments with visible light irradiation were performed at ambient temperature of *ca*. 20 °C using a 150 W metal halide lamp as the light source. To limit the irradiation wavelength, the light beam was passed through a 410 nm cut filter (L41) to ensure the cut-off wavelengths shorter than 410 nm. Then, samples of the suspension were withdrawn after a definite time interval, and the residual MO concentration was analyzed using a UV-vis spectrophotometer (UV762, Shanghai Analysis Co).

Results and Discussion

Characterization of Ce/TiO_2/ACF photocatalyst

The BET surface areas and pore volumes of the catalysts are summarized in Table 1. As shown in Table 1, the porous structure of the ACF was significantly altered after Ce/TiO_2 loading. The specific surface area (S_{BET}) was reduced from 985.6 to 513.7 m^2/g and total pore volume was reduced from 0.563 to 0.392 cm^3/g. This indicates that the pores of the ACF were blocked considerably by the loaded Ce/TiO_2.

The SEM micrographs of the pure ACF and Ce/TiO_2/ACF photocatalyst calcined at 500 ºC are shown in Fig. 1. It was observed that the fibers are 10-20 μm in diameter and have many unbroken axial grooves on the surface. The coating of Ce/TiO_2 particles was by and large evenly distributed on the outer surfaces of the fibers with scattered aggregates of Ce/TiO_2. The surface Ce/TiO_2 coating has an important role in the photocatalytic reaction since most of it would be photon accessible. Therefore, using ACF as the support, Ce/TiO_2 can maximize

Table 1 — Physicochemical properties of ACF and Ce/TiO_2/ACF

Sample	S_{BET} (m^2/g)	Total pore vol. (cm^3/g)	Band gap energy (eV)
ACF	985.6	0.563	—
Ce/TiO_2/ACF	516.2	0.399	3.21
0.10 mol% Ce/TiO_2/ACF	515.5	0.397	3.06
0.20 mol% Ce/TiO_2/ACF	513.7	0.392	2.83
0.30 mol% Ce/TiO_2/ACF	521.1	0.402	2.97

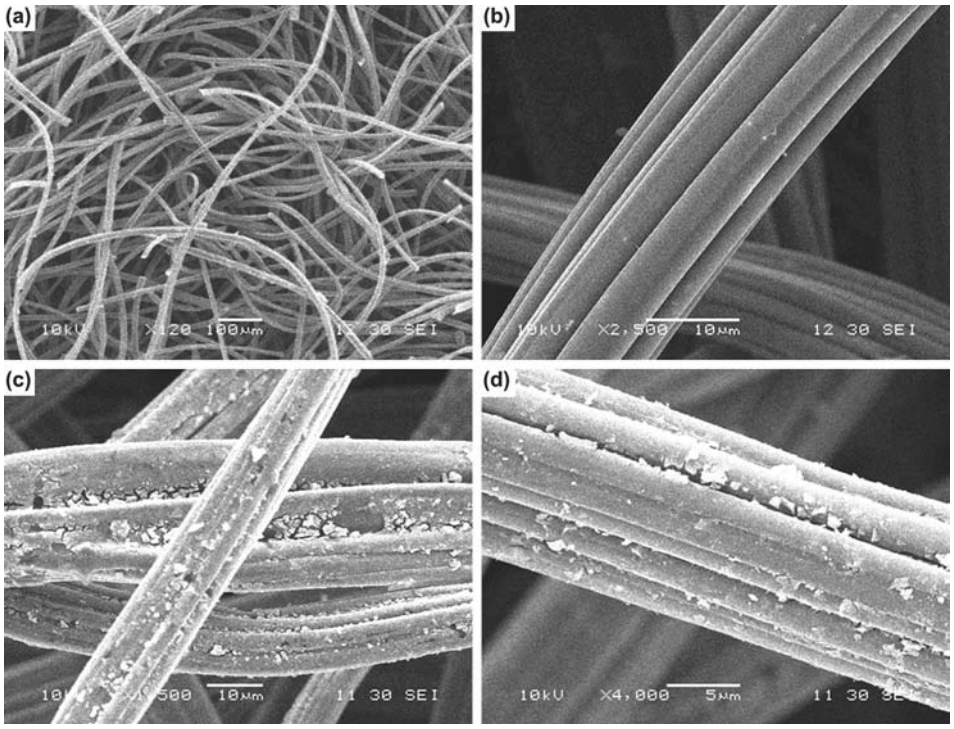

Fig. 1 – SEM photographs of pure ACF and 0.20 mol%Ce/TiO_2/ACF photocatalyst. [(a) ACF, 120x; (b) ACF, 2500x; (c) Ce/TiO_2 coating on ACF, 1500x; (d) Ce/TiO_2 coating on ACF, 4000x].

photon available catalytic surface compared to granular activated carbon, zeolite, etc.

X-ray diffraction patterns of the pure ACF and Ce/TiO_2/ACF photocatalyst calcined at 500 ºC are shown in Fig. 2. The broad diffraction peak at 43.6º of the pure ACF is attributed to the reflections from both (1 0 0) and (1 0 1) planes of graphite[24]. While the calcination temperature increased up to 500 ºC, this typical peak still appeared in the XRD patterns of the Ce/TiO_2/ACF photocatalyst. This indicates that the micrographic structure of ACF has not been damaged by Ce/TiO_2 deposition and calcination at high temperatures. The diffraction peaks at 25.28°, 37.80°, 48.05° and 55.07° are consistent with the (1 0 1), (0 0 4), (2 0 0) and (1 0 5) peaks of anatase TiO_2. XRD pattern of the Ce/TiO_2/ACF photocatalyst shows that the photocatalyst has anatase structure, with no significant rutile component. The XRD results also suggest that the Ce-doping has no influence on the nature of crystal formation. No characteristic peak of Ce oxide was found in the XRD patterns, implying that either the Ce ions were incorporated in the crystallinity of TiO_2 or that the Ce oxide was very small and highly dispersed.

UV-vis absorption spectra were used to characterize the light absorption ability of the prepared photocatalysts. The absorption spectra for Ce/TiO_2/ACF samples with different Ce-doping concentrations are shown in Fig. 3. The absorption in the region between 420 and 650 nm for the photocatlysts is shifted to a longer wavelength as compared to undoped TiO_2/ACF. The absorption reaches a maximum for the sample with 0.20 mol% Ce. Further increase in the Ce-doping concentration results in the shifting of absorption curves towards the shorter wavelength. For pure TiO_2, the absorption in the ultraviolet range (λ = 378 nm) is associated with the excitation of the O 2*p* electron to the Ti 3*d* level. The red shift of the absorption spectrum can be ascribed to the charge transfer between the TiO_2 valence or conduction band and the Ce ion 4*f* level[25]. Band gap energies (Eg) of the prepared photocatalysts calculated by the formula $Eg = 1239.8/\lambda g$ are listed in Table 1. For pure TiO_2 prepared without any dopant, the Eg was 3.21 eV. In the case of Ce-doped TiO_2, Eg decreased from 3.06 to 2.83 eV, depending on the dopant content. The lowest Eg (2.83 eV) was observed for 0.20 mol% Ce-doped TiO_2 sample (see Table 1). The narrowing of band gaps of the prepared Ce-doped TiO_2 may be due to the interaction of TiO_2 with Ce in lower oxidation state, suggesting that the prepared Ce-doped TiO_2 is responsive to the visible light. Moreover, since the rare earth elements possess a broad absorption band, the effect of their incorporation into the TiO_2 is similar to adding a photosensitizer to the reaction solution. Therefore, the Ce ions surrounding the TiO_2 grains can absorb a larger range of light radiation, which brings about the higher light absorption in the 420–650 nm region of the Ce-doped TiO_2/ACF[26]. This extended absorbance indicates the possible enhancement in the photocatalytic activity of TiO_2/ACF illuminated by visible light.

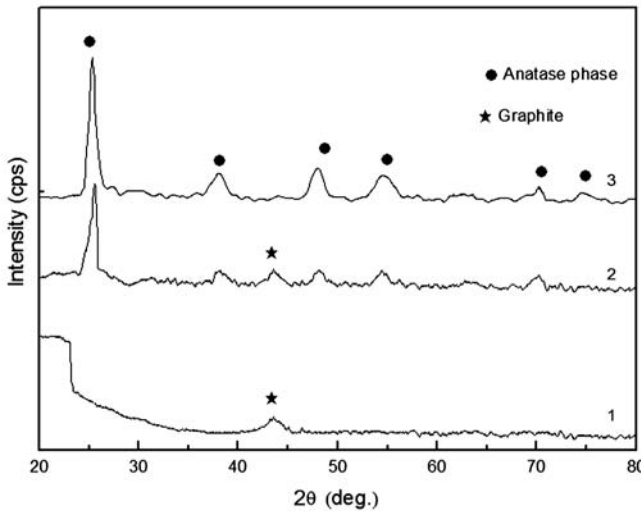

Fig. 2 – XRD patterns of ACF and catalyst samples. [1, ACF; 2, 0.20 mol% Ce/TiO_2/ACF; 3, TiO_2].

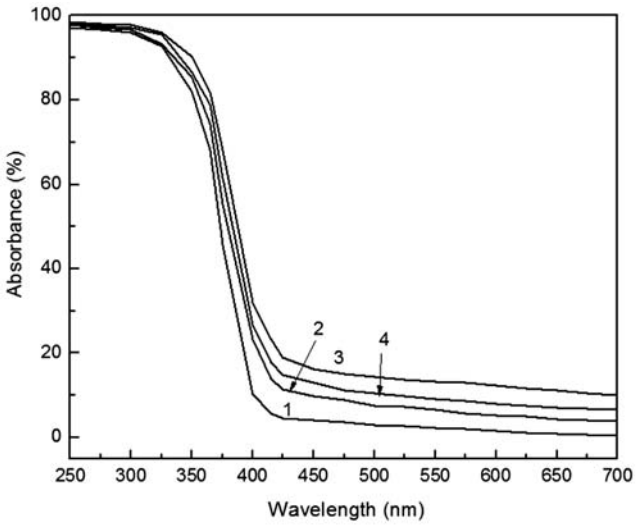

Fig. 3 – UV-vis absorption spectra of catalyst samples. [1, TiO_2/ACF; 2, 0.10 mol% Ce/TiO_2/ACF; 3, 0.20 mol% Ce/TiO_2/ACF; 4, 0.30 mol% Ce/TiO_2/ACF].

Effect of Ce-doped content on the photocatalytic activity of Ce/TiO_2/ACF

Figure 4 shows the MO degradation with irradiation time under UV irradiation in the presence of Ce/TiO_2/ACF with cerium doped content in the range of 0.10–0.30 mol%. It is shown that the photocatalytic activity of TiO_2/ACF is enhanced after cerium doping and the optimum content of cerium is 0.20 mol%. The presence of cerium on TiO_2/ACF is considered to influence the photoreactivity by altering the electron-hole pair recombination rate through the following processes[15]:

$$Ce^{4+} + e^- \rightarrow Ce^{3+} \quad \ldots (1)$$

$$Ce^{3+} + O_2 \rightarrow O_2^{\bullet -} + Ce^{4+} \quad \ldots (2)$$

Thus, it can be seen that the Ce 4*f* level in Ce/TiO_2/ACF plays an important role in interfacial charge transfer and inhibition of electron-hole recombination. The increase in the photocatalytic activity with the increase in the content of cerium doping may be attributed to the electrons trapped in cerium sites, which are subsequently transferred to the absorbed O_2. The photoactivity of Ce/TiO_2/ACF increases gradually with increase in cerium doping up to 0.20 mol%. However, the photoactivity of Ce/TiO_2/ACF decreases when the content of cerium doping reaches 0.30 mol%. This indicates that on heavy doping the dopants become recombination centers of the photoexcited electrons, thus reducing the photocatalytic activity. Consequently, it is understandable that there is an optimum value of cerium doping. It is proposed that the presence of Ce ions on the TiO_2 influences the photocatalytic activity by creating oxygen vacancies, which generates low energy states at the bottom of the conduction band and serves as electron trap sites in nanocrystalline TiO_2. The low energy states introduced by rare earth ion in the top valence band also serve as hole trap sites[27]. The separation of the charge carriers is attributed to such trapping. Subsequently, the charge carriers transfer to the surface of photocatalyst initiating redox reactions, and thereby promoting photocatalytic activity of Ce-doped TiO_2.

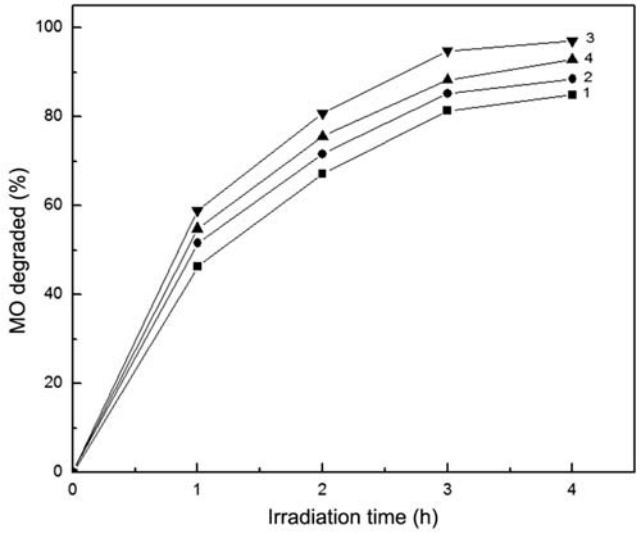

Fig. 4 – Effect of Ce-doped content on the degradation rate of MO. [1, TiO_2/ACF; 2, 0.10 mol% Ce/TiO_2/ACF; 3, 0.20 mol% Ce/TiO_2/ACF; 4, 0.30 mol% Ce/TiO_2/ACF].

The UV-vis absorption spectra show that cerium doping improves photo-utilization of TiO_2/ACF, and generating more electron-hole pairs under light irradiation, which helps to improve the photocatalytic activity of TiO_2/ACF. At the same time, rare earth elements have the ability of oxygen storage; they can also release oxygen to the reaction systems, when the concentration of oxygen in the system is low[28]. It is known from the photocatalytic mechanism that oxygen adsorbed on the photocatalyst can trap the photogenerated electron effectively[29], and hence inhibit the simple recombination between electron and hole, enhancing the photocatalytic activity.

Photocatalytic activity

Photocatalytic activity of the prepared samples was estimated by measuring the degradation rate of MO in the presence of UV and visible light irradiations, without considering the degradation intermediates in detail. Pure TiO_2 synthesized by the same method was used as the reference system. In order to evaluate the actual photocatalytic activity of the 0.20 mol% Ce/TiO_2/ACF photocatalyst calcined at 500 ºC for 2 h, the six MO degradation processes, viz., photolysis of MO, photocatalytic degradation of pure ACF, TiO_2, TiO_2/ACF, 0.20 mol% Ce/TiO_2/ACF and adsorption of 0.20 mol% Ce/TiO_2/ACF, were compared by assessing the effect of catalyst on the overall removal rate for an initial MO concentration of 50 mg/L (Fig. 5).

Experimental results show that MO is degraded a little under UV light irradiation without the catalyst (Fig. 5, curve 1). The adsorption of MO on pure ACF is saturated after 60 min under UV light irradiation, and the concentration of MO does not decrease any further on prolonging of UV light irradiation time. This indicates that the pure ACF does not have photocatalyst activity (Fig. 5, curve 2). Similarly, 0.20 mol% Ce/TiO_2/ACF

shows no photocatalytic activity without irradiation of UV light (Fig. 5, curve 3). The MO degradation rates increase with increasing UV light irradiation time for the MO/TiO_2, MO/TiO_2/ACF and MO 0.20 mol% Ce/TiO_2/ACF systems, but the decomposition percentages of MO with 0.20 mol% Ce/TiO_2/ACF are much higher than with TiO_2 and TiO_2/ACF (Fig. 5, curves 4, 5, 6). By comparison of the amounts of MO removed with and without 0.20 mol% Ce/TiO_2/ACF (Fig. 5), it is affirmed that the disappearance of MO molecules was due to photocatalytic degradation by Ce/TiO_2/ACF.

Figure 6 shows the results of MO degradation with varying irradiation time under visible light in the presence of different photocatalysts. Experimental results show that the percentage of MO degraded is less under visible light irradiation for the MO/TiO_2/ACF system. The MO degradation rates increases with increasing visible light irradiation time for the MO/Ce/TiO_2/ACF system, corresponding to the maximum red shift in the UV-vis absorption spectra (Fig. 3). The percentage of MO degraded of Ce/TiO_2/ACF is found to be almost four times higher than that of TiO_2/ACF. This is in agreement with the results of the outcome from the optical absorption spectra analysis.

Recyclability of the 0.20 mol% Ce/TiO_2/ACF catalyst

In order to test the recyclability of the 0.20 mol% Ce/TiO_2/ACF photocatalyst, the photocatalytic degradation experiments of MO were repeated for four cycles (Supplementary Data, Fig. S1). The photocatalytic activity of the photocatalyst was only slightly reduced in the stirred aqueous solution, up to four cycles, and the photocatalytic activity of 0.20 mol% Ce/TiO_2/ACF remained *ca.* 86.5% of the activity of the as-prepared sample after being used four times. The degradation percentage of MO reached 84.6% when irradiation time was 4 h. Thus, it is proposed that the deposited Ce/TiO_2 is firmly attached to the ACF surface, and is not easily exfoliated from the ACF in the mechanically stirred solutions for a long period. At the same time, this also indicates that the final removal of MO from the solution was caused by the photocatalytic degradation of MO on the photocatalyst. These results indicate that cyclic usage of the Ce/TiO_2/ACF was possible and its stability in treating polluted water was satisfactory. Therefore, it is potentially employable for continuous photocatalytic degradation processes.

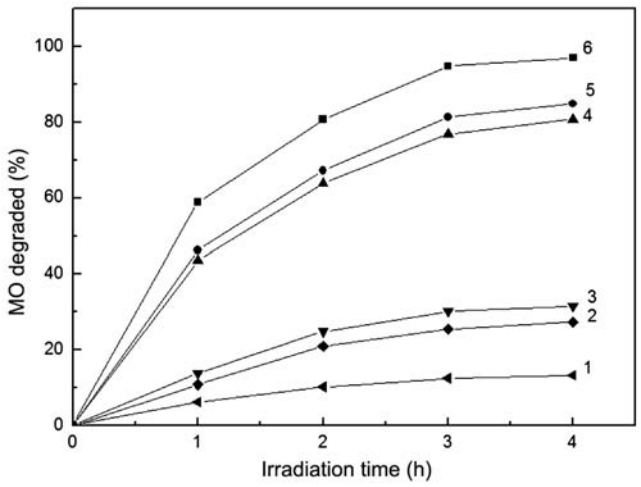

Fig. 5 – Degradation curves of MO with UV light irradiation time. [1, photolysis of MO; 2, ACF in presence of UV light; 3, 0.20 mol% Ce/TiO_2/ACF in absence of UV light; 4, TiO_2 in presence of UV light; 5, TiO_2/ACF in presence of UV light; 6, 0.20 mol% Ce/TiO_2/ACF in presence of UV light].

Kinetics of MO photodegradation

The photocatalytic degradation of MO was studied at initial concentration of 50 mg/L. The residual concentration of MO in the aqueous 0.20 mol% Ce/TiO_2/ACF suspension under UV light irradiation can be obtained from Fig. 5 (curve 6). As expected, the concentration of MO decreased exponentially during irradiation. The results can be described by a first order kinetic model $\ln C_0/C_t = kt$, where C_t is the concentration of MO in solution at irradiation time t and k is the first order rate constant. Linear plot of $\ln C_t$ versus irradiation time t was obtained, from which slopes k can be estimated,

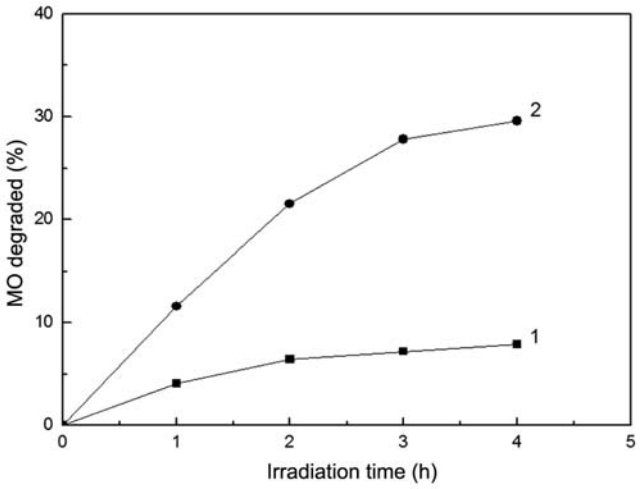

Fig. 6 – Degradation curves of MO with visible light irradiation time. [1, TiO_2/ACF in presence of visible light; 2, 0.20 mol% Ce/TiO_2/ACF in presence of visible light].

indicating that the photocatalytic degradation of MO can be reasonably described by first order kinetic model. The coefficients of the first order kinetic model obtained from the linear plot of ln C_t versus irradiation time t gave the observed first order rate constant (k) value to be 0.9146 h^{-1} and the squared correlation coefficient (R^2) as 0.9917, which show that the kinetics of MO photodegradation is first order reaction.

Conclusions

A visible light-driven photocatalyst (Ce/TiO_2/ACF) was prepared by supporting photoactive cerium-doped titanium dioxide on activated carbon fibers via hydrolysis of tetrabutyl titanate with ammonium ceric nitrate in the presence of activated carbon fibers. Ce-doping enhanced the photocatalytic activity of TiO_2/ACF under UV and visible light irradiation, with the 0.2 mol% Ce-doped sample exhibiting the optimum photocatalytic activity for MO degradation. Ce-doping caused the absorption spectra of TiO_2/ACF to shift to the visible region. The photocatalyst could be used repeatedly and the photocatalytic degradation properties were maintained with only a slight decline. Therefore, the combination of Ce/TiO_2 and ACF is a promising material for application in degradation of MO.

Supplementary Data

Supplementary data associated with this article, viz., Fig. S1, is available in the electronic form at http://www.niscair.res.in/jinfo/ijca/IJCA_53A(06)665-671_SupplData.pdf.

Acknowledgement

The authors gratefully acknowledge financial support for this work from the National Natural Science Foundation of China, PR China, (41373127) and Liaoning Provincial Natural Science Foundation of China, PR China (2013020121).

References

1 Ao C H, Lee S C, Yu Y Z & Xu J H, *Appl Catal B*, 54 (2004) 41.
2 Ochuma I J, Fishwick R P, Wood J & Winterbottom J M, *J Hazard Mater*, 144 (2007) 627.
3 Strini A, Cassese S & Schiavi L, *Appl Catal B*, 61(2005) 90.
4 Thompson T & Yates J T, *Chem Rev*, 106 (2006) 4428.
5 Rachel A, Subrahmanyam M & Boule P, *Appl Catal B*, 37 (2002) 301.
6 De Vos D E, Dams M, Sels B F & Jacobs P A, *Chem Rev*, 102 (2002) 3615.
7 Wang C, Böttcher C, Bahnemann D W & Dohrmann J K, *J Nanopart Res*, 6 (2004) 119.
8 Zhang W, Li Y, Zhu S & Wang F, *Catal Today*, 93-95 (2004) 589.
9 Sun B, Reddy E P & Smirniotis P G, *Appl Catal B*, 57 (2005) 139.
10 Xu J, Lu M, Guo X & Li H, *J Mol Catal A*, 226 (2005) 123.
11 Wu J C & Chen C H, *J Photochem Photobiol A*, 163 (2004) 509.
12 Ghorai T K, Dhak D, Biswas S K, Dalai S & Pramanik P, *J Mol Catal A*, 273 (2007) 224.
13 Ghorai T K, Dhak D, Dalai S & Pramanik P, *Mater Res Bull*, 43 (2007) 1770.
14 Baiju K V, Sibu C P, Rajesh K, Krishna Pillai P, Mukundan P, Warrier K G K & Wunderlich W, *Mater Chem Phys*, 90 (2005) 123.
15 Xie Y & Yuan C, *Appl Catal B*, 46 (2003) 251.
16 Yao S H, Jia X Y, Jiao L L, Zhu C & Shi Z L, *Indian J Chem* 51A (2012) 1049.
17 Liu Z L, Guo B, Hong L & Jiang H, *J Phys Chem Solids*, 66 (2005) 161.
18 Horikoshi S, Watanabe N, Onishi H, Hidaka H & Serpone N, *Appl Catal B*, 37 (2002) 117.
19 Uddin M J, Cesano F, Bonino F, Bordiga S, Spoto G, Scarano D & Zecchina A, *J Photochem Photobiol A*, 189 (2007) 286.
20 Yao S H, Jia Y F & Zhao S L, *Environ Technol*, 33 (2012) 983.
21 Bideau M, Claudel B, Dubien C, Faure L & Kazouan H, *J Photochem Photobiol A*, 91 (1995) 137.
22 Bozzi A, Yuranova T, Guasaquillo I, Laub D & Kiwi J, *J Photochem Photobiol A*, 174 (2005) 156.
23 Körösi L & Dékány I, *Colloids Surf A*, 280 (2006) 146.
24 Matsumoto A, Tsutsumi K & Kaneko K, *Langmiur*, 8 (1992) 2515.
25 Lin J & Yu J C, *J Photochem Photobiol A*, 116 (1998) 63.
26 Gao Y, Xu A W & Zhu J Y, *Chinese J Catal*, 22 (2001) 53.
27 Shi J W, Zheng J T, Hu Y & Zhao Y C, *Mater Chem Phys*, 106 (2007) 247.
28 Yamada T, Kayano K & Funabiki M, *Stud Surf Sci Catal*, 77 (1993) 329.
29 Gerischer H & Heller A, *J Phys Chem*, 95 (1991) 5261.